




Toward automated irrigation management with integrated crop water stress index and spatial soil water balance

Sandeep Bhatti¹ · Derek M. Heeren²  · Susan A. O'Shaughnessy³ · Christopher M. U. Neale⁴ · Jacob LaRue^{5,6} · Steve Melvin⁷ · Eric Wilkening² · Geng Bai²

Accepted: 25 May 2023 / Published online: 3 July 2023
© The Author(s) 2023

Abstract

Decision support systems intended for precision irrigation aim at reducing irrigation applications while optimizing crop yield to achieve maximum crop water productivity (CWP). These systems incorporate on-site sensor data, remote sensing inputs, and advanced algorithms with spatial and temporal characteristics to compute precise crop water needs. The availability of variable rate irrigation (VRI) systems enables irrigation applications at a sub-field scale. The combination of an appropriate VRI system along with a precise decision support system would be ideal for improved CWP. The objective of this study was to compare and evaluate two decision support systems in terms of seasonal applied irrigation, crop yield, and CWP. This study implemented the Spatial EvapoTranspiration Modeling Interface (SETMI) model and the Irrigation Scheduling Supervisory Control and Data Acquisition (ISSCADA) system for management of a center pivot irrigation system in a 58-ha maize-soybean field during the 2020 and 2021 growing seasons. The irrigation scheduling methods included: ISSCADA plant feedback, ISSCADA hybrid, common practice, and SETMI. These methods were applied at irrigation levels of 0, 50, 100, and 150% of the full irrigation prescribed by the respective irrigation scheduling method. Data from infrared thermometers (IRTs), soil water sensors, weather stations, and satellites were used in the irrigation methods. Mean seasonal irrigation prescribed was different among the irrigation levels and methods for the 2 years. The ISSCADA plant feedback prescribed the least irrigation among the methods for majority of the cases. The common practice prescribed the largest seasonal irrigation depth among the methods for three crop-year cases. The maize yield in rainfed was found to be significantly lower than the irrigated levels in 2020 since 2020 was a dry year. No significant differences were observed in crop yield among the different irrigation methods for both years. The CWP among the different irrigation methods ranged between 2.72 and 3.15 kg m⁻³ for 2020 maize, 1.03 and 1.13 kg m⁻³ for 2020 soybean, 3.57 and 4.24 kg m⁻³ for 2021 maize, and 1.19 and 1.48 kg m⁻³ for 2021 soybean. Deficit level (50%) had the largest irrigation water productivity in all crop-year cases in this study. The ISSCADA and SETMI systems were found to reduce irrigation applications as compared to the common practice while maintaining crop yield. This study was the first to implement the newly developed integrated crop water stress index (iCWSI) thresholds and the ISSCADA system for site-specific irrigation of maize and soybean in Nebraska.

Keywords Crop water productivity · Decision support system · Variable rate irrigation · Thermal sensing · Evapotranspiration · Center pivot irrigation

Introduction

Precision irrigation aims for improved CWP by managing spatiotemporal crop water requirements in a field. Recent advances in sensing technologies, data processing systems, modeling approaches, and communication protocols facilitate the management of site-specific irrigation at a sub-field scale (O’Shaughnessy et al., 2019). Over the past decade, numerous precision irrigation technologies and methodologies have been developed and tested across different cropping systems (Barker et al., 2019; Bhatti et al., 2020; Haghverdi et al., 2016; Lena et al., 2020; Mendes et al., 2019; O’Shaughnessy et al., 2015; Osroosh et al., 2016; Stone et al., 2020; Sui & Yan, 2017; Taghvaeian et al., 2014; Thorp, 2020; Vories et al., 2020). While there is an abundance of precision irrigation tools, it is important to assess the suitability of these irrigation scheduling methods in terms of CWP, complexity, and economic viability (O’Shaughnessy et al., 2019). The downsides of precision irrigation include associated costs and lack of effective algorithms and real-time availability of data for irrigation scheduling (Evetts et al., 2020a, 2020b, 2020c). Currently, site-specific irrigation systems are primarily utilized by producers to avoid application on non-arable areas of the field (Evans et al., 2013). The potential benefits include improved CWP, reduced leaching, and energy savings, which are yet to be demonstrated (Lo et al., 2016).

Uniform rate irrigation and speed control VRI are easier to manage than zone control VRI and have the potential of incorporating sensor data and precision irrigation techniques for improving CWP. The flow rate of individual sprinklers along the lateral pipe does not vary with location in case of uniform rate or speed control VRI. Integrated sensing systems, advanced modeling tools, and irrigation scheduling algorithms will be beneficial for both site-specific and conventional irrigation methods (Thorp et al., 2022). Data streams for precision agriculture require temporal and spatial knowledge of soil, plant, and field characteristics. Precision irrigation technologies should be centered on plant water relations in the soil–plant–atmosphere–continuum for sustainable management of irrigation water (Zhang et al., 2021). Precision irrigation tools using sensor data integration, remote sensing inputs, and modeling approaches, have shown promise as effective decision support systems for irrigation management.

Crop water stress can be estimated spatially and temporally using systems such as the ISSCADA system, which was developed and patented (Evetts et al., 2014) by the USDA Agricultural Research Service in Bushland, TX. This system uses iCWSI to schedule irrigation and monitor crop water stress in the field. The iCWSI is computed by integrating the crop water stress index (Jackson et al., 1981) estimated for every minute between the daylight hours. Continuous measurement of canopy temperature is needed at different locations across the field to compute spatial iCWSI maps for the field. The spatial canopy temperature measurements can be obtained by mounting IRTs on moving irrigation systems (O’Shaughnessy et al., 2015, 2017, 2020; Evetts et al., 2020b; Sui et al., 2017). A scaling algorithm was developed to estimate diurnal temperatures from data collected by the pivot-mounted IRTs by using stationary IRTs as a reference (Peters & Evetts, 2004). The diurnal time series data are estimated using a one-time-of-day temperature reading taken during daylight hours (moving IRT sensors) and an equation that scales the temperature to a known reference temperature curve (measurements from the stationary sensors). In this

way, diurnal temperature time series were determined for many footprint areas in the field. The diurnal temperature time series data are used to compute spatial iCWSI for the field and automate irrigation management using the ISSCADA system (O’Shaughnessy et al., 2012). The ISSCADA system was found to adequately manage irrigation scheduling at a site-specific level in different climates (O’Shaughnessy et al., 2017; Stone et al., 2020; Sui et al., 2020; Vories et al., 2020). This system has built-in algorithms to convert weather, soil water sensing, and canopy temperature data into reliable irrigation decisions and automate the management of moving center pivot irrigation systems.

The SETMI model (Geli & Neale, 2012; Neale et al., 2012) has the ability to estimate spatial crop water requirements and manage precision irrigation. Multiyear studies on site-specific irrigation were conducted using the SETMI model for maize and soybean in Nebraska (Barker et al., 2018, 2019; Bhatti et al., 2020). This model combines a reflectance-based crop coefficient evapotranspiration approach (water balance approach) with a two-source energy balance approach (Norman et al., 1995). The water balance approach computes the soil adjusted vegetation index (SAVI; Huete, 1988) from red and near-infrared bands and uses the relationships between basal crop coefficients and SAVI (Campos et al., 2017). The energy balance approach uses thermal infrared imagery to compute the latent heat flux and estimate crop evapotranspiration (ET) at a spatial scale. Sensor-based soil water measurements from the root zone can also be used to update the water balance in the SETMI model (Bhatti et al., 2020). The water balance approach can forecast irrigation needs using historic weather data, which can prove beneficial to producers. The ISSCADA system and SETMI model have never been implemented on the same field in a research experiment for comparing their potential in site-specific irrigation management.

The overall goal of the study was to implement two decision support systems for site-specific irrigation management and compare the crop yield and water productivity for maize and soybean in eastern Nebraska. The ISSCADA system used in-situ and ground-based proximal thermal sensing data, and the SETMI model used satellite imagery with neutron probe soil water data to compute crop water requirements. These precision irrigation methods were compared with the common irrigation scheduling method practiced by farmers in the area. The specific objectives included: (1) the comparison of different irrigation methods applied at four different irrigation levels in terms of crop yield and irrigation applied, (2) the assessment of CWP and two other water productivities among the different treatments, and (3) the investigation of the suitability of newly developed iCWSI thresholds for irrigation management of maize and soybean in eastern Nebraska.

Material and methods

Experimental site and design

The study was conducted on a 58-ha maize-soybean research field located at the University of Nebraska’s Eastern Nebraska Research and Extension Center, NE, U.S.A. (centered at 41.172445°N, 96.478248°W) during the 2020 and 2021 growing seasons (Bhatti et al., 2022a). The field was irrigated using a seven-span, speed control enabled center pivot irrigation system (lateral length of 400 m), model Valley Irrigation 8000 (Valmont, Valley, NE), with the X-Tec center drive motors (capable of making a revolution in about 4 h). The sprinklers on the pivot lateral were Nelson spinners (model S3030, Nelson, Walla Walla, WA) installed on drops at a height of about 2.4 m from the ground and with a sprinkler

spacing of 2.7 m. The field was divided into north and south halves managed under a maize-soybean rotation (Fig. 1). The soils in the field were classified as silt loam and silty clay loam (gSSURGO, Soil Survey Staff, 2018). The planting and harvesting dates were April 24 and October 13 for maize 2020, May 2 and September 28 for soybean 2020, April 28 and October 8 for maize 2021, and May 13 and October 21 for soybean 2021, respectively. Anhydrous ammonia injection applications were applied uniformly after the soybean harvest in the north half in 2020.

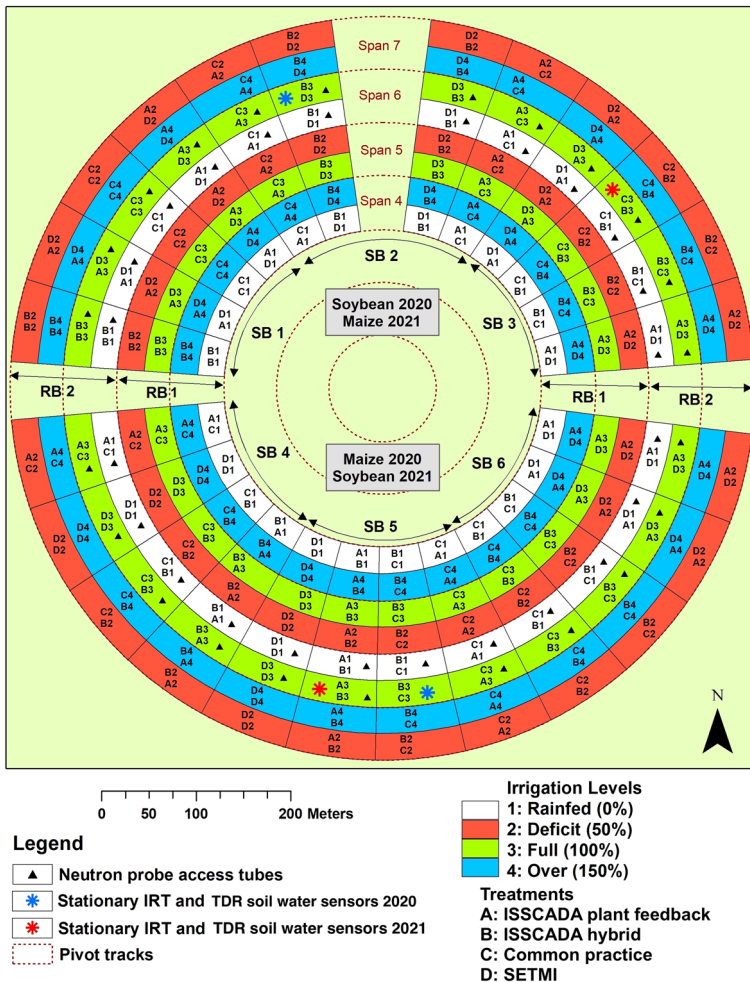


Fig. 1 Layout of experimental plots for 2020 and 2021 growing seasons. The irrigation methods included: A for ISSCADA plant feedback, B for ISSCADA hybrid, C for common practice, and D for SETMI. The irrigation levels were depicted by different color rings and included: 1 for Rainfed, 2 for Deficit, 3 for Full, and 4 for over. The irrigation method-level combinations were mentioned in each plot, where the upper row was 2020 label, and the lower row was 2021 label. Neutron access tubes, stationary soil water and IRT stations, and center pivot tire tracks were marked on the map. Labels ‘RB 1–2’ stands for radial blocks 1 and 2, and labels ‘SB 1–6’ stands for sector blocks 1 through 6. Outer four center pivot spans were also labeled in the figure. The IRTs mounted on the center pivot lateral were not marked on this map since they moved as the center pivot moved across the field

A total of 192 plots were designed for the field using eight radial zones (concentric zones) and 24 arc-wise plot boundaries (Fig. 1). The area under the outer four spans of the pivot was used for the experiment. The north and south halves had a total of 96 plots each. The plots were approximately rectangular with lengths ranging between 43 and 90 m, and a constant width of 28 m. The area of the plots ranged between 1205 m² and 2630 m². There were a total of 16 treatment combinations: four irrigation scheduling methods, and four irrigation levels. Each combination of an irrigation method-level had six replicates for each crop. The treatments were assigned to the experimental plots using a strip-block design with two treatment factors: irrigation scheduling methods and irrigation refill levels. More details on the different scheduling methods and refill levels are provided in the section ‘Irrigation management’ below. The 24 arc-wise sectors (14° sector angle) were assigned to six sector blocks with three sector blocks in each crop: west, center, and east sector blocks (Fig. 1). Each sector block included four arc-wise sectors, which were randomly assigned with the four irrigation scheduling methods. The eight radial zones (concentric zones shown in different colors in Fig. 1) were assigned to two radial blocks, and each radial block constituted two pivot spans. The inner four radial zones were assigned to radial block 1 and outer four radial zones were assigned to radial block 2. These radial zones were randomly assigned with four irrigation levels for each radial block. The irrigation methods were randomized between the four arc-wise sectors within each sector block for the second year of the study. In 2021, the irrigation levels were not randomized among radial blocks due to logistical reasons (needed reconfiguration of sprinkler nozzles).

Experimental data

Thermal sensing

The canopy temperature was sensed using IRTs (model SAP-IP IRT, Dynamax, Inc., Houston, TX, USA) mounted on stationary posts and on brackets mounted on the center pivot lateral. The spectral range of the IRT was 8–14 μm with a 20° field of view. The outer two spans of the center pivot were used to mount eight IRTs: two IRTs each for the four irrigation levels. Each pair of IRTs were mounted about 6.1 m from the edges of the respective radial zone borders and pointed towards the center of the zone at oblique angles to nadir (see more details in Bhatti et al., 2022b). The IRTs were mounted on the pivot at a height of about 3.6 m from the ground using special mounting arms secured to the truss rods, which extended the field of view of the IRTs by about 3 m ahead of the pivot lateral when moving in the forward/clockwise direction.

Stationary IRTs were installed near the centroid of one ISSCADA hybrid-full plot for each crop. These sensors were positioned at a nadir view angle and the height was manually adjusted to maintain a distance of about 1 m above the canopy. When the maize reached maximum crop height, the 1 m spacing between the sensor and maize canopy could not be maintained since the sensor height had to remain below the truss level to prevent damage. After this timeframe, the sensor height was between 0.3 and 0.5 m higher than the tassel of maize. The maximum height of the stationary IRT from the soil surface was about 3 m for maize and about 2.2 m for soybean. The data from the IRTs were recorded every five seconds and were averaged over 1 min. The 1 min data were transmitted using the wireless Zigbee communication protocol at a frequency of 2.54 GHz to a coordinator (model IRT-COR, Dynamax, Inc., Houston, TX, USA). The coordinator routed the data through a USB connection to an embedded computer (model MXE-1401, Adlink Technology, Inc.,

San Jose, California USA) at the center pivot point. The embedded computer also had a serial connection to the CAMS (control) panel of the center pivot system and collects time-stamped data including the GPS location of the end-tower, the center pivot speed, pressure and voltage. A separate software system (ARSPivot) was installed on the embedded computer to download data from a nearby AgSense weather station and manages the data collected from the IRT network, the CAMS panel, distributed wireless network of the soil water sensors (discussed below), and the AgSense weather station to build a prescription map (Andrade et al., 2020).

The center pivot system was moved around the field without water (dry scan) to collect data using the pivot mounted IRTs. A total of 16 dry scans in 2020 and 19 dry scans in 2021 were conducted to sense spatial canopy temperature data. The dry scans were mainly conducted between 10:00 AM and 5:30 PM. The scaling algorithm (Peters & Evett, 2004), incorporated in the ARSPivot software, was used by the ISSCADA system to estimate the diurnal canopy temperature for each one-time of day remote measurement recorded by each pair of IRTs mounted on the pivot lateral. Additionally, the algorithm uses a reference measurement from a stationary IRT to capture diurnal pattern in canopy temperature at one location in the field. Further, the algorithm scales the diurnal canopy temperature curve from stationary IRT to a predicted temperature curve for a remote location using ratio between the reference temperature and the remote location measurement, referenced to the predawn temperature (Peters & Evett, 2004). There were about 180 remote locations or canopy temperature measurements that were monitored by one moving IRT mounted on the pivot in a dry scan conducted at 100% speed. Data from the stationary IRTs were used to develop a reference temperature curve in the scaling algorithm. The integrated crop water stress index (iCWSI; O'Shaughnessy et al., 2020) was also computed by the ISSCADA system at each remote location for every minute during daylight hours from 9:00 AM to 7:00 PM. The iCWSI was computed using following equation as mentioned in O'Shaughnessy et al. (2017):

$$iCWSI = \sum_{i=1}^N \frac{(T'_c - T_a) - (T_c - T_a)_{ll}}{(T_c - T_a)_{ul} - (T_c - T_a)_{ll}} \quad (1)$$

where i is the i^{th} time step, N is total number of 1 min steps between 9:00 AM and 7:00 PM, T'_c is canopy temperature estimated using scaling algorithm, T_a is ambient air temperature, $(T_c - T_a)_{ll}$ represents the lower limit of the canopy and air temperature differential, and $(T_c - T_a)_{ul}$ represents the upper limit of the canopy and air temperature differential. The lower and upper limits of the canopy temperature and air temperature difference were computed using the theoretical approach (Jackson et al., 1981). The weather variables required for computing the upper and lower limits were acquired from an onsite AgSense weather station. All computations were automatically conducted by the ISSCADA system at midnight following a dry scan.

A separate data analysis of the thermal data using iCWSI (Bhatti et al., 2022a) demonstrated that crop water stress could be detected before incurring crop yield loss. This was possible in a narrow range when the photosynthesis rate (and carbon assimilation) was limited by solar radiation (energy-limiting water stress), yet the leaf had abundant carbon dioxide for photosynthesis. In non-irrigated plots, the water stress progressed and stomatal conductance further decreased until photosynthesis was limited by carbon dioxide (carbon-dioxide-limiting water stress), in which case a yield reduction occurred (Fig. 2). A significant increase in daily carbon gain by a soybean plant was found when stomatal conductance and soil water content was high in the more recently released cultivars (Koester et al., 2016). Hence, the canopy temperature and stomatal conductance will vary with different

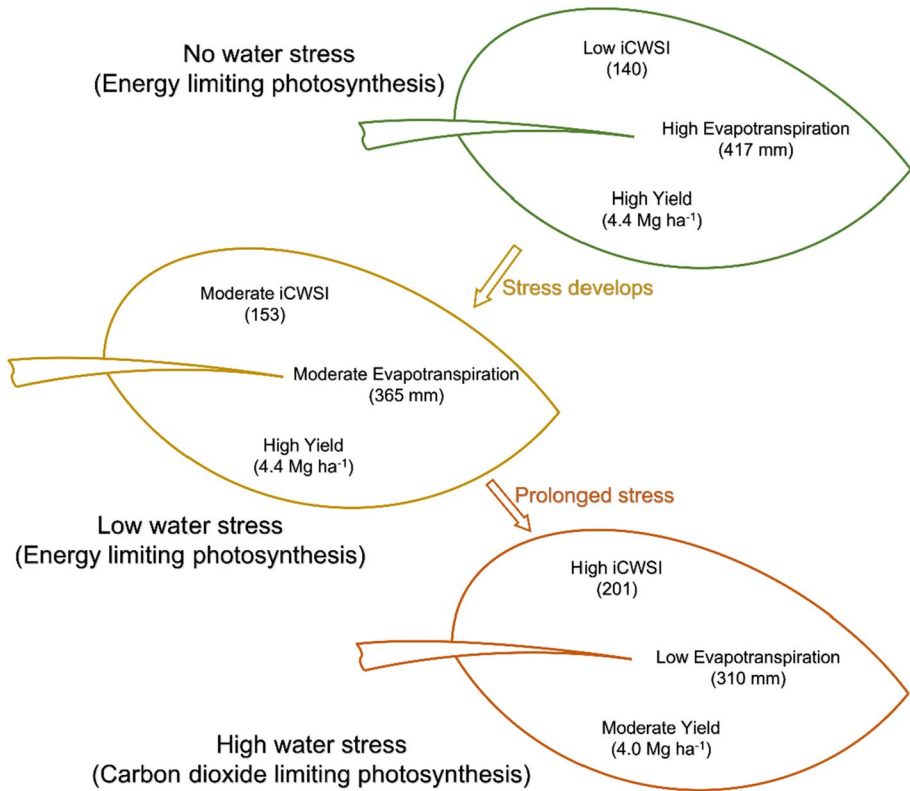


Fig. 2 Schematic of three conditions of water stress supported by data for integrated crop water stress index, evapotranspiration, and crop yield from soybean in 2020 (adapted from Bhatti et al., 2022a)

cultivars and affect the carbon gained by the plant. More research is warranted on the energy limiting stress with different cultivars.

Soil water sensing

A total of eight time-domain reflectometer (TDR) soil water sensors (model TDR315L, Acclima, Inc., Meridian, Idaho, USA) were installed horizontally at four depths (0.15, 0.30, 0.46, and 0.76 m) in two hybrid plots (one location per crop; Fig. 1). The four depths were selected to represent soil water profile of the root zone to a depth of 1 m. Three sensors were installed within 0.5 m of the ground surface to capture the dynamic nature of soil water in shallow depths. The soil water stations consisting of four TDR sensors were situated adjacent to the stationary IRTs in the same plot. The data was sensed at a frequency of 15 min and stored using a CR300 datalogger with an embedded RF407 radio (Campbell Scientific, Logan, Utah, USA). The data were transmitted wirelessly using the proprietary PakBus communication protocol and Yagi antennas (Campbell Scientific) operating at 900 MHz. Data were collected using a RF407 radio serving as a base station modem connected to the embedded computer.

Soil water data from two neutron probes (model 503 Elite Hydroprobe, CPN, Concord, CA) were also monitored at multiple depths including 0.15, 0.46, 0.76, and 1.07 m. Since the representative volume of a soil water measurement from neutron probe is larger compared to TDR sensors, the depths of measurement for neutron probe were equally spaced to represent soil water profile to a depth of 1.2 m. The data were collected with a frequency of about 3 weeks. For each crop, 24 access tubes were installed in the approximate geometric center of each plot with 12 tubes each in the rainfed and full levels (Fig. 1). Field calibration from a nearby site (3 km away) with the same soils was used for one of the probes (Bhatti et al., 2020). The second probe was cross-calibrated using the first probe for the field site.

Remote sensing imagery

Remote sensing data was acquired from the PlanetScope satellite multispectral imager (Planet Labs, Inc., San Francisco, CA, USA) with a spatial resolution of 3 m and temporal resolution of ~1 day. The imagery was captured over the field between 10:30 and 11:30 AM. The data were only selected if the imagery over and around the field was free of clouds and image stripes. A total of 20 images (taken between May 8 and October 10) in 2020, and 27 images (taken between April 29 and October 18) in 2021 were used in SETMI. The model used the red and near-infrared bands of the multispectral imagery to compute the SAVI.

Weather data

A weather station (AgSense, Valmont Industries, Inc., Huron, SD, USA) was installed in an open area located to the west of the field. The weather data included air temperature, relative humidity, wind speed and direction, solar radiation, and rainfall, which were collected at a frequency of 5 min. The suite of sensors included a cup anemometer, wind direction sensor, pyranometer, relative humidity sensor, air temperature sensor, and rain gauge (model Vantage Pro2 Plus, Davis Instruments, Hayward, CA). The cup anemometer was mounted at a height of about 3 m. The weather data was automatically retrieved by the ISSCADA system and was also accessible manually through the AgSense website. In addition, weather data was also acquired from Memphis 5N weather station (Automated Weather Data Network, High Plains Regional Climate Center), which was about 5 km from the field. Historic 20-yr weather data (2000–2019) was also accessed from this weather station to compute the normal reference ET.

Crop yield

Crop yield was calculated using yield monitor data from the combine harvesters. The yield data was cleaned and processed using the Yield Editor software version 2.0 (USDA-Agricultural Research Service, Columbia, MO). The processed data was then checked using the mean yield reported from the weighing grain carts. The Yield Editor software was used to adjust the moisture of grains (measured using yield monitor) to 15.5% for maize and 13% for soybean. The dry yield was computed by removing the mass of moisture from the grains (dry yield = (100 – percent moisture in grain) * yield). Data points were only included if they were within a 6.1 m buffer from each plot boundary.

Irrigation management

The values of field capacity and wilting point used were $0.4 \text{ m}^3 \text{ m}^{-3}$ and $0.2 \text{ m}^3 \text{ m}^{-3}$, respectively. These values were computed by averaging field capacity and wilting point measurements from multiple locations in a nearby field (within 3 km; Bhatti et al., 2020). The irrigation depths prescribed in an irrigation event ranged between 5 and 25 mm. The different irrigation refill levels included rainfed, deficit, full, and over-applied at 0, 50, 100, and 150%, respectively of the amounts determined by each irrigation scheduling method for the full level. Hence, the 50 and 150% levels were computed by scaling the full irrigation amount by corresponding fractions. Since the center pivot was not capable of varying the irrigation rate of individual sprinklers on the pivot lateral, the sprinkler nozzles for the deficit and over levels were outfitted with the required sized nozzles to achieve variable rate application along the lateral of the pivot. These custom sized nozzles for the deficit and over levels were specified by the irrigation dealer for achieving the required application depth in the respective irrigation zones. The nozzles for the deficit level were switched to smaller sizes (to achieve 50% of the full), and the nozzles for the over level were changed to larger sizes (to achieve 150% of the full). The nozzles for the rainfed zone were set to the off position, so these nozzles applied no water throughout the season. The sprinkler nozzles automatically applied corresponding amounts of irrigation on the respective irrigation levels (0, 50, 100, and 150%). With these modifications to the sprinkler package from the default manufacturer's design, system uniformity analysis was conducted using catch-can tests to ensure high application efficiency in the different management zones. Two catch-can tests were conducted on June 25, 2020, and June 10, 2021. The wind speed, air temperature, and time for the test were 4.5 m s^{-1} , $30 \text{ }^\circ\text{C}$, and 12:00 PM–1:00 PM, respectively, in 2020 and 2.6 m s^{-1} , $31 \text{ }^\circ\text{C}$, and 10:00–11:00 AM, respectively, in 2021. Average percent difference between measured (in cans) and prescribed irrigation depth was 28% in 2020 and 13% in 2021. The test in 2021 was conducted early in the morning with lower evaporative demand and lower wind speeds than 2020. The Christiansen uniformity coefficient (CU) was also determined for each irrigation level following Eisenhauer et al. (2021). The CU in the deficit level was 53% for 2020 and 71% for 2021. The CU for the over level was 82% for 2020 and 92% for 2021. The full level had a CU of above 90% in both tests. To account for boundary effects from neighboring management zones, a buffer of 6.1 m from each plot boundary was used. The plot area after excluding the buffer zone was used to prescribe irrigation. The input irrigation depth for each sector was determined using the four irrigation methods discussed below.

ISSCADA plant feedback method

The iCWSI data were calculated for each treatment plot. Canopy temperature data from dry scans were only used for iCWSI computations. It was found that the canopy temperature collected during irrigation events had an apparent canopy cooling of about $2 \text{ }^\circ\text{C}$ from irrigation water for this sprinkler configuration due to the wet canopy (Bhatti et al., 2022b). Therefore, the canopy temperature data collected during irrigation was not used for computing iCWSI. The iCWSI data for each plot designated as “plant feedback method with the full level” computed by the ISSCADA system from the most recent dry scan were compared with pre-established iCWSI thresholds that were used to determine the irrigation amount. The most recent dry scan IRT data was used to schedule irrigation in 2021. The replicate plots of this method in different sector blocks were managed independent of

each other and had varying levels of irrigation prescribed in a single irrigation event. This method included three iCWSI thresholds: low (L), medium (M), and high (H) threshold. These thresholds are region, climate, and crop specific.

For irrigation management in 2020, the iCWSI data for a dry scan were compared among the different irrigation levels to compute the prescribed irrigation depth. The minimum iCWSI values for the rainfed and deficit levels were used as the high threshold. The minimum iCWSI values from the full level plots were used as the low threshold. The average value of the high and low thresholds was used as the medium threshold. The most recent dry scan data were used to compute new thresholds for each irrigation event in 2020. The low, medium, and high thresholds used for 2020 ranged between 100 and 150, 130 and 170, and 150 and 190, respectively, for both crops. These thresholds were used to determine the amount of irrigation in 2020. The timing of the irrigation was decided based on soil water data from the Acclima TDR sensors similar to the hybrid method. The thresholds for irrigation management for the 2021 growing season were computed using the iCWSI data from the 2020 growing season (refer to Bhatti et al., 2022a for details). The low, medium, and high thresholds were 120, 150, and 180, respectively for maize and 110, 130, and 150, respectively for soybean. The irrigation was prescribed according to the mean iCWSI calculated for the designated treatment plots: no irrigation for $iCWSI \leq L$, 13 mm for $L < iCWSI \leq M$, 19 mm for $M < iCWSI \leq H$, and 25 mm for $iCWSI > H$. It was observed that the mean iCWSI computed for rainfed was always higher as compared with deficit or full irrigation levels. Hence, it was more likely that the irrigation would be triggered using iCWSI thresholds for rainfed since the iCWSI values for rainfed were higher in comparison with the other levels (Bhatti et al., 2022a).

ISSCADA hybrid method

The ISSCADA hybrid method used the soil water data from TDR soil water sensors and iCWSI data collaboratively to prescribe irrigation. The depth weighted average of soil water content was used to represent root zone soil water content. The soil water depletion (SWD) was estimated from the field capacity, wilting point, and soil water content (O'Shaughnessy et al., 2020). The ratio of SWD to the maximum value of SWD (difference between field capacity and wilting point) was used to define SWD thresholds. The irrigation was managed with SWD and iCWSI thresholds: if $SWD \leq 15\%$ then no irrigation, if $15\% < SWD \leq 35\%$ then manage using only iCWSI thresholds as in plant feedback method, and if $SWD > 35\%$ then apply 25 mm irrigation. The most recent dry scan iCWSI data and SWD values computed using TDR sensors from the hybrid-full treatment plots were used to manage irrigation for this method. The iCWSI data for each hybrid-full treatment plot were independently used to prescribe irrigation for the plot. However, one value of SWD was used for this method at a given time since there was one location of TDR sensors per crop.

SETMI method using spatial evapotranspiration model

The water balance approach of the spatial evapotranspiration model was used to prescribe irrigation for the SETMI method (Neale et al., 2012). This approach maintains a seasonal water balance for the crop which is updated with remote sensing imagery on a regular basis. The model was input with PlanetScope imagery, and SAVI was computed at 3 m pixel resolution using red and near-infrared bands. The crop ET was computed using the

dual crop coefficient approach (Allen et al., 1998) and reflectance-based crop coefficients (Campos et al., 2017; Neale et al., 2012). The model estimated water balance components on a daily basis. The water balance was updated with inputs of rainfall and irrigation. The modeled root zone was linearly increased from 0.1 to 1 m between the respective dates of crop emergence, and maximum crop coefficient. The SWD computed with the model was updated using soil water data from the neutron probe. Neutron probe data from three different SETMI-full plots for each crop were used to adjust the SWD. Depth weighted soil water content was used to compute representative soil water content for the root zone. The SWD adjustment was conducted following the methodology described in Bhatti et al. (2020). The model forecasted crop water requirements using normal reference crop ET computed from the 20-year historic weather data and forecasted crop coefficients for the entire season. The forecasted crop water requirements were used to apply irrigation for the upcoming week. A management allowable depletion (MAD) threshold was used for scheduling irrigation in order to maintain soil water above MAD. The MAD was used as 50% of the available water capacity (difference between soil water content at field capacity and wilting point) for majority of the season, which was increased to 60% for both crops late in the season (around denting stage for maize and appearance of yellow leaves in soybean). The crop water requirements were computed at 3 m resolution, and pixels excluding a 6.1 m inner buffer from each plot boundary were averaged to compute the prescribed irrigation depth for the plot. The inner buffer for each plot was used to remove any boundary effects from adjacent plots. Additional model specific details can be found in Bhatti et al., 2020. The two-source energy balance approach of the model was not implemented due to time and logistical constraints.

Common practice

This method represented the common practice for irrigation scheduling in eastern Nebraska. An agronomist prescribed irrigation by sampling soil up to 0.6 m using a soil probe in a common practice-full treatment plot. The hand feel method was used on a weekly basis to feel the soil wetness and texture to make conclusions on irrigation requirements. In cases of hot and dry weather with high evapotranspiration, the field was sampled for soil water estimation two times during a week. The prescribed irrigation with this method was always 25 mm in the full irrigation level. This method allowed for the comparison of sensor-driven irrigation methods with the common practices in the area.

Irrigation application

The prescribed irrigation depths for each method were uploaded to the center pivot system using the AgSense remote management tool. The angles for each sector and corresponding irrigation depths were entered in the AgSense software. The different depths of irrigation among the different sectors were achieved by varying the speed of the pivot, given the constant flow rate and operating pressure through the individual sprinklers. A single value of irrigation depth was entered for each sector in the AgSense software, and varying depths of irrigation were applied in each sector with the custom-sized nozzles. The ISSCADA system has the ability to upload and run irrigation prescriptions through the center pivot. However, the ISSCADA system was set up as a zone control system on a speed control pivot. The zone control configuration of the ISSCADA system enabled data collection and computation of iCWSI for each treatment plot independently. Therefore, the AgSense tool

was used for irrigation management, and the ISSCADA system was used for data collection and crop water stress computations. The ISSCADA system was successfully deployed for irrigation management on August 4, 2020. The irrigation on the ISSCADA treatments before August 4 were prescribed similar to the common treatment. The ISSCADA system was used to prescribe four irrigation prescriptions after August 4 for each crop in 2020.

Data analysis

Seasonal irrigation, crop yield, and water productivity were compared among all the treatment plots. The seasonal irrigation and crop yield were statistically tested to identify differences among the treatments at a 5% significance level. Statistical analysis was computed using SAS 9.4 (SAS Institute, Inc., Cary, NC) software. PROC GLIMMIX was used to run the univariate analysis of variance (ANOVA). The main effects of methods and levels along with the interaction between the methods and levels were used in the model statement. The blocking was treated as a random effect for these tests. Two blocking effects including radial blocks and sector blocks, were considered in the model. The irrigation water productivity (IWP), evapotranspiration water productivity (ETWP), and CWP were expressed in kg m^{-3} and computed following Evett et al., (2020a, 2020b, 2020c):

$$IWP = \frac{Y_i - Y_d}{I_i}$$

$$ETWP = \frac{Y_i - Y_d}{ET_i - ET_d}$$

$$CWP = \frac{Y}{ET}$$

where Y is dry yield (kg m^{-2}), I is applied irrigation depth (m), and ET is actual crop evapotranspiration (m). Subscripts i and d represents variables corresponding to irrigation treatment i , and dryland treatment d , respectively. Statistical differences in IWP among the treatments were also computed at a 5% level. The ET data was only available for a few plots in the full and rainfed level plots. Hence, there were inadequate replicates to compute statistical differences for ETWP and CWP. The ET were computed using neutron probe measurements, water balance components computed from SETMI, and seasonal water inputs (rainfall or irrigation). More details on ET computations can be found in Bhatti et al. (2022a).

The relationship between irrigation applied and crop yield was also computed using plot values of irrigation and yield. These relationships were used to study the increase in yield per unit increase in water application for different plots. It was hypothesized that the over level plots will not produce significantly larger yield as compared with the full level plots.

Eliminated data

The yield data for soybean in the north half in 2020 indicated significant differences between the east and west quarters. The irrigation prescriptions did not have significant differences in water application between east and west quarters. The average yield in the west quarter was 4.7 Mg ha^{-1} and in the east quarter was 4.1 Mg ha^{-1} . The plot yield in the east

quarter was consistently lower than the west quarter for different irrigation treatments. The reason for this difference in yield is unclear, and no such observation was found in yield maps from the past 5 years. As a result of this observed difference in yield between the two quarters, 36 plots from sector block 2 (Fig. 1) which were split equally between east and west quarters had to be eliminated from yield analysis in 2020. The eliminated plots could have resulted in mean yield for two methods (present in the west quarter for sector block 2) to be significantly larger than the other two methods (present in the east quarter for sector block 2). The yield data for maize in 2020 or for both crops in 2021 did not demonstrate any differences in yield data between the east and west quarters.

Results and discussion

Seasonal climate

The 2020 and 2021 growing seasons were different from each other in terms of the seasonal rainfall received. The cumulative rainfall between June and September was 178 mm for 2020 and 386 mm for 2021. The depth of rainfall was almost double in 2021. Historic average rainfall (1991–2020) from June to September was 381 mm for the Mead 6S station (National Centers for Environmental Information), which was about 6.5 km southwest of the field. Therefore, 2020 was a dry season when compared with the normal historic rainfall. The average daily air temperature between June and September was 12.3 °C for 2020, and 13.1 °C for 2021. The maximum air temperature on average was larger in 2021 (29.2 °C) as compared to 2020 (28.9 °C). The average relative humidity was 58% for both years. Solar radiation was slightly larger in 2020 (549 W/m²) as compared to 2021 (541 W/m²). Wind speed was similar for both years on average (3.5 m/s in 2020 and 3.2 m/s in 2021).

Seasonal soil water depletion and water inputs

The rainfall, SWD, and irrigation were depicted using a representative plot for all crop-year cases (Fig. 3). A plot assigned with the full level and SETMI method was selected for each crop-year. The SWD was modeled on a daily basis for the entire season using SETMI and corrected using soil water data from the neutron probe. The MAD was also plotted as a reference to the SWD. The modeled root zone was linearly increased from 0.1 to 1 m for this model run. This resulted in a constant increase of the MAD from the early to peak developmental stage (identified as the date when crop coefficients reached maximum value) for each crop. The SWD on average indicated an increase with time, but the root zone depletion did not reach the allowable depletion (Fig. 3). It is evident that the frequency and magnitude of rainfall events were much higher in 2021 as compared with the 2020 season. The 2021 season had seven rainfall events larger than 25 mm as compared to only one event in 2020. Several large rainfall events were observed after August 6, 2021, and only one irrigation event was applied after this day for each crop.

Seasonal prescribed irrigation depth

The mean seasonal prescribed irrigation depth was compared among the different treatment plots (Table 1). The mean seasonal irrigation depth reported in Table 1 was

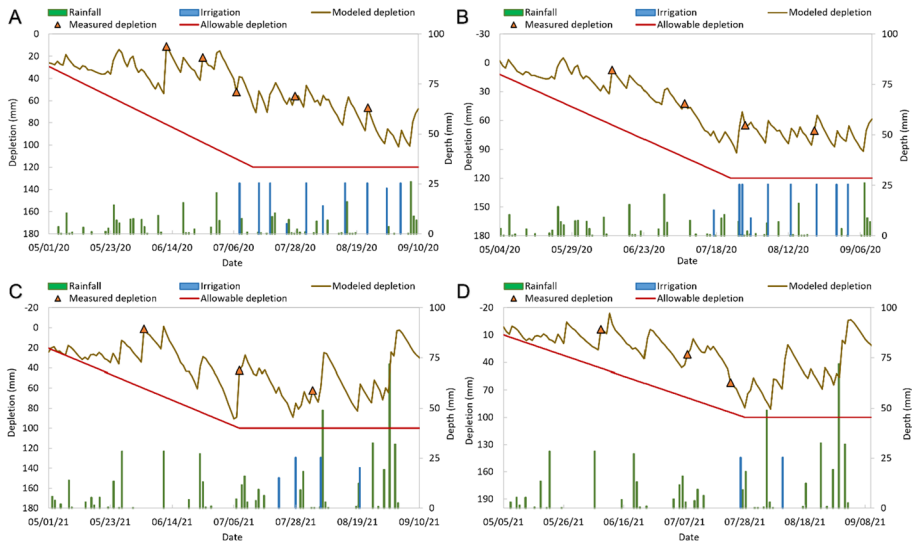


Fig. 3 Seasonal soil water depletion, rainfall, and irrigation for a representative full level plot in **A** maize 2020, **B** soybean 2020, **C** maize 2021, and **D** soybean 2021. Soil water depletion was modeled using SETMI and updated with neutron probe soil water data. Management allowable depletion and soil water depletions were plotted using the left vertical axis. The rainfall and irrigation events were plotted using the right vertical axis

computed as the average total irrigation depth prescribed during the growing season (April–October) for all plots under an irrigation treatment. This depth was reported for all irrigation levels and methods (Table 1). The mean irrigation depth for a specific irrigation level was computed by averaging irrigation applied for the four irrigation methods. Further, the mean irrigation depth for a specific irrigation method was computed using the average irrigation depth applied in plots with 50, 100, and 150% levels.

There were a total of 11 and 10 irrigation events applied in maize and soybean, respectively, between July 2 and September 3 of the 2020 growing season. There were four irrigation events prescribed for both crops after the implementation of ISSCADA for irrigation management in 2020. In 2021, there were five and four irrigation events applied in maize and soybean, respectively, between July 10 and August 20. As a consequence of the experimental setup, the irrigation depths among the different irrigation levels were always significantly different from each other for both years. This observation was expected as the irrigation depths were applied at 50, 100, and 150% of the irrigation depth prescribed by each irrigation method for the deficit, full, and over levels, respectively. In 2020, the range of mean seasonal irrigation depth for plots with the four methods applied at the full level was 37 and 41 mm for maize and soybean, respectively. The seasonal irrigation averaged for the irrigated levels was largest for the common method (254 mm) in maize, and for the ISSCADA hybrid and SETMI methods (203 mm) in soybean. The mean seasonal irrigation depth for SETMI method (219 mm) was significantly smaller than those of the other irrigation methods for maize (Table 1). For soybean, the ISSCADA plant feedback (172 mm) and common practice (178 mm) methods were significantly smaller in seasonal irrigation than the other two methods. The full level plots averaged for all methods were prescribed with 236 mm for maize, and 189 mm for soybean on average.

Table 1 Least square means of irrigation depth, crop yield, and water productivities computed for different irrigation treatments applied to maize and soybean during 2020 and 2021

Treatment	Irrigation (mm)	Yield (Mg ha ⁻¹)	IWP (kg m ⁻³)	CWP (kg m ⁻³)	ETWP (kg m ⁻³)
Maize 2020 levels					
Rainfed	–	11.8 b	–	4.01	–
Deficit	118 c	13.1 a	1.12 a	–	–
Full	236 b	13.7 a	0.77 b	2.98	1.19
Over	354 a	13.7 a	0.52 c	–	–
Maize 2020 methods excluding rainfed					
Plant feedback	227 c	13.6 a	0.91 a	3.09	1.37
Hybrid	241 b	13.4 a	0.72 a	2.94	1.12
Common	254 a	13.4 a	0.73 a	2.72	0.83
SETMI	219 d	13.5 a	0.85 a	3.15	1.42
Soybean 2020 levels					
Rainfed	–	4.0 a	–	1.4	–
Deficit	94 c	4.4 a	0.34 a	–	–
Full	189 b	4.4 a	0.21 a	1.1	0.36
Over	283 a	4.5 a	0.16 a	–	–
Soybean 2020 methods excluding rainfed					
Plant feedback	172 b	4.3 a	0.12 a	1.03	0.21
Hybrid	203 a	4.6 a	0.28 a	1.13	0.61
Common	178 b	4.5 a	0.30 a	1.08	0.21
SETMI	203 a	4.5 a	0.26 a	1.11	0.43
Maize 2021 levels					
Rainfed	–	14.6 a	–	4.3	–
Deficit	46 c	14.8 a	0.58 a	–	–
Full	92 b	15.0 a	0.43 a	3.88	0.79
Over	138 a	14.8 a	0.19 a	–	–

Table 1 (continued)

Treatment	Irrigation (mm)	Yield (Mg ha ⁻¹)	IWP (kg m ⁻³)	CWP (kg m ⁻³)	ETWP (kg m ⁻³)
Maize 2021 methods excluding rainfed					
Plant feedback	59 d	14.8 a	0.58 a	4.24	1.06
Hybrid	95 b	14.7 a	0.20 a	3.82	0.7
Common	127 a	15.0 a	0.40 a	3.57	0.54
SETMI	87 c	14.9 a	0.40 a	3.82	0.74
Soybean 2021 levels					
Rainfed	–	5.0 a	–	1.4	–
Deficit	28 c	4.9 a	–0.17 a	–	–
Full	56 b	4.9 a	–0.05 a	1.29	0.49
Over	84 a	5.0 a	0.10 a	–	–
Soybean 2021 methods excluding rainfed					
Plant feedback	46 b	5.0 a	0.12 a	1.19	0.06
Hybrid	25 c	5.0 a	0.15 a	1.48	1.84
Common	102 a	4.9 a	–0.05 a	1.12	0.08
SETMI	51 b	4.8 a	–0.38 a	1.32	0.02

The IWP, CWP, and ETWP stands for irrigation water productivity, crop water productivity, and evapotranspiration water productivity, respectively. The letters next to the values denote statistical differences among the irrigation methods or levels for different crop-year combinations

In 2021, the range of seasonal irrigation among all plots with the four methods applied at the full level was 70 and 76 mm for maize and soybean, respectively. The seasonal irrigation was significantly larger for the common practice method than other methods for both crops (127 mm for maize and 102 mm for soybean). The plant feedback method had minimum irrigation for maize (59 mm), and the hybrid method had minimum irrigation for soybean (25 mm). The range in prescribed irrigation among the full level plots in 2021 was much larger than in 2020 for both crops even though the overall irrigation applied in 2021 was comparatively smaller. The full level plots were prescribed with 92 mm for maize, and 56 mm for soybean on average. There was a significant interaction between the methods and levels for prescribed irrigation in 2021. For soybean, the common method applied at 100% was larger in prescribed irrigation than the other methods applied at 150%. For maize, the plant feedback method applied at 150% was significantly smaller than the common method applied at 100%. Prescriptions generated by the ISSCADA and SETMI methods for the full level plots on July 2, 2022 were indicated in Fig. 4. It was observed that the ISSCADA plant feedback method on this day prescribed irrigation depth between 13 and 19 mm as compared to 15 mm prescribed by the SETMI method and 25 mm prescribed by the ISSCADA hybrid method.

Crop yield

The mean crop yield data for both crops were compared among the irrigation methods and levels (Table 1). The irrigation applied and crop yield data for all individual treatments (four irrigation methods with four irrigation levels) are depicted in Fig. 5. In 2020, the average maize yield was only found to be significantly lower for rainfed (11.8 Mg ha^{-1}) as compared to the other irrigation levels. The full and over levels had a mean yield of 13.7 Mg ha^{-1} , and deficit had a mean yield of 13.1 Mg ha^{-1} . There were no significant differences found in maize yield among the irrigation methods. The soybean yield was not found to be significantly different among the methods and levels. Rainfed had a mean soybean yield of 4 Mg ha^{-1} , which was lower than the other irrigation levels ($4.4\text{--}4.5 \text{ Mg ha}^{-1}$). This yield difference between rainfed and other irrigation levels was found to be not significant. The elimination of soybean yield data from 32 plots reduced the power of the statistical test which could be a reason for this yield difference to be non-significant. The mean soybean yield among the methods ranged between 4.3 Mg ha^{-1} in plant feedback and 4.6 Mg ha^{-1} in hybrid.

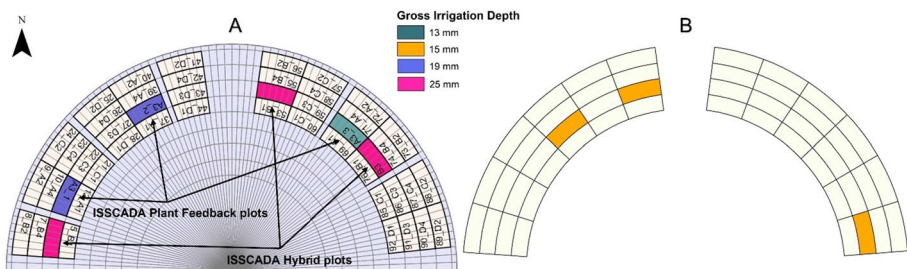


Fig. 4 Irrigation prescriptions generated for full level plots on July 2 in 2022 by **A** ISSCADA plant feedback and hybrid methods, **B** SETMI model

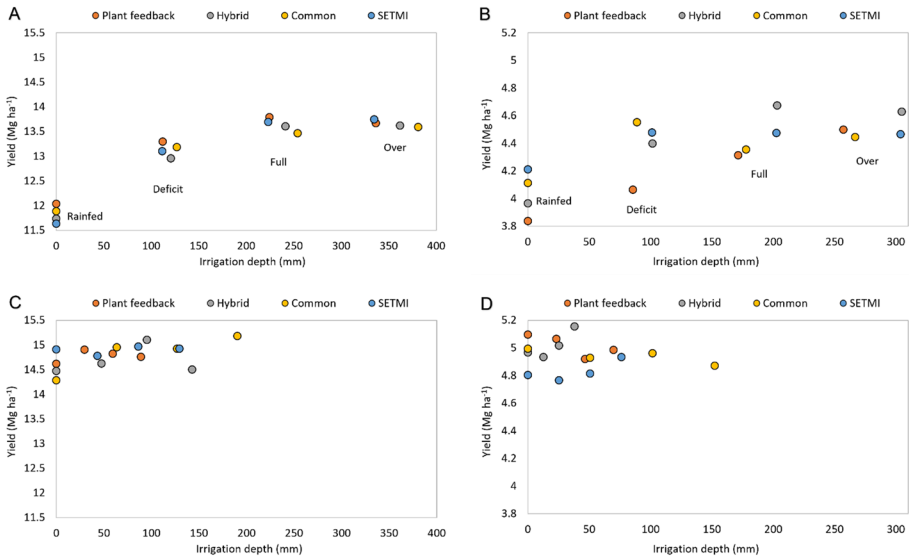


Fig. 5 Mean irrigation depth vs. crop yield plotted for different method-level combinations for **A** maize 2020, **B** soybean 2020, **C** maize 2021, and **D** soybean 2021. Each sub-figure contains 16 data points corresponding to the 16 method-level combinations (4 irrigation methods applied at 4 irrigation levels)

In 2021, mean yield differences were not significant among both the levels and the methods for both crops. The rainfed had a similar crop yield as compared to the irrigated treatments. Since the rainfall in 2021 was much larger than in 2020, the rainfed crop had optimal yield similar to irrigated crop in 2021. The mean maize yield among the levels ranged between 14.6 Mg ha⁻¹ in rainfed and 15 Mg ha⁻¹ in the full level. The mean maize yield among the methods was between 14.7 Mg ha⁻¹ in hybrid and 15.0 Mg ha⁻¹ in common. The soybean yield ranged between 4.8 and 5 Mg ha⁻¹ among the different levels and methods. There were no significant interactions found between the main effects of methods and levels. The computed iCWSI thresholds from 2020 season data were used for scheduling irrigation in the ISSCADA treatments in 2021. There were three irrigation events triggered using the iCWSI thresholds for each crop in 2021. The optimal yield and reduced irrigation application (compared to the common practice) observed in the ISSCADA treatments indicated that the iCWSI thresholds worked well for the 2021 growing season for both crops. These thresholds should be further tested during a few dry seasons in this region to validate their credibility for irrigation management of maize and soybean.

Crop water productivity

The statistical differences in IWP were computed for both crops in 2020 and 2021 (Table 1). For maize in 2020, the IWP ranged between 0.52 kg m⁻³ (over) and 1.12 kg m⁻³ (deficit) among the irrigation levels. The IWP among the levels were significantly different from each other. The deficit level had the largest IWP among the levels. There were no significant differences in IWP for maize among the methods, which ranged between 0.72 kg m⁻³ in hybrid and 0.91 kg m⁻³ in plant feedback. The IWP ranged between 0.16 kg m⁻³ in over and 0.34 kg m⁻³ in deficit for soybean in 2020. The IWP differences

among the irrigation levels were not significant for soybean. Among the methods, the common practice had the maximum IWP of 0.3 kg m^{-3} , and plant feedback had the minimum IWP of 0.12 kg m^{-3} . In 2021, no significant differences were observed in IWP among the levels and the methods for both crops. The IWP among the irrigation levels ranged between 0.58 kg m^{-3} in deficit and 0.19 kg m^{-3} in over for maize. This range was from 0.2 kg m^{-3} in hybrid and 0.58 kg m^{-3} in plant feedback among the irrigation methods. For soybean, the range in IWP was from -0.17 kg m^{-3} in deficit to 0.1 kg m^{-3} in over among the levels. The minimum and maximum IWP among the methods were -0.38 kg m^{-3} in SETMI and 0.15 kg m^{-3} in hybrid. The negative values of IWP were observed in 2021 due to few irrigation applications and optimal yield produced in the rainfed crop. The IWP was found to be largest in deficit among the different levels in all cases except soybean in 2021. The plant feedback and hybrid methods were found to have the largest IWP for maize and soybean, respectively in both years. In contrast, a study in Stoneville, Mississippi yielded an IWP between 1.33 and 2.49 kg m^{-3} for maize during the 2014 and 2015 growing seasons (Sui & Yan, 2017). They also found that the IWP for soybean ranged between 0.48 and 1.2 kg m^{-3} in 2014 and 2015. Another irrigation study on corn conducted in Florence, South Carolina from 2016 to 2019 found IWP values between -1.8 and 3.2 kg m^{-3} (Stone et al., 2020). In particular, they found that the IWP for the plant feedback method ranged between -1.8 and 3.2 kg m^{-3} , and for the hybrid method ranged between 1.58 and 2.64 kg m^{-3} during the study period.

The CWP and ETWP were also computed from the ET and yield data (Table 1). The CWP was computed for rainfed and full levels only. Evapotranspiration data was not available for deficit and over levels. The rainfed level had larger CWP as compared to the full level in all cases. The full level had a CWP of 2.98 kg m^{-3} in 2020 and 3.88 kg m^{-3} in 2021 for maize. In an earlier study, the average CWP for maize was found to range between 1.61 kg m^{-3} in 2013 and 2.1 kg m^{-3} in 2014 for maize in Bushland, Texas (O'Shaughnessy et al., 2017). The maximum CWP for maize was found in the SETMI method (3.15 kg m^{-3}) in 2020 and in the plant feedback method (4.24 kg m^{-3}) in 2021. The maximum CWP for soybean was observed in hybrid for both years (1.13 kg m^{-3} in 2020 and 1.48 kg m^{-3} in 2021). The maize ETWP for the full level was 1.19 kg m^{-3} in 2020 and 0.79 kg m^{-3} in 2021. In 2020, the maize ETWP ranged between 0.83 kg m^{-3} in common practice and 1.42 kg m^{-3} in SETMI. The soybean ETWP ranged between 0.21 kg m^{-3} (plant feedback and common practice) and 0.61 kg m^{-3} (hybrid). In 2021, the maize ETWP ranged between 0.54 kg m^{-3} (common practice) and 1.06 kg m^{-3} (plant feedback). The soybean ETWP ranged between 0.02 kg m^{-3} in SETMI and 1.84 kg m^{-3} in hybrid. In summary, the SETMI and plant feedback methods in 2020 and 2021, respectively had the largest ETWP for maize, and the hybrid method had the largest ETWP for soybean in both years.

Irrigation production function

An irrigation production function was computed using irrigation and crop yield data for each irrigation treatment (Fig. 5). It was observed that the data points for each level were differentiable from each other in 2020, and data labels were placed next to the cluster for each level in the figure. An apparent increase in maize yield was observed with the rainfed, deficit, and full level clusters in 2020 (Fig. 5). There was no increase in maize yield between the full and over levels. The increase in soybean yield between the rainfed and full levels was not obvious in 2020. The data from sector block two (32 plots) were eliminated for soybean 2020. In 2021, there were no significant yield differences among the

treatments. It can be seen from Fig. 5 that the irrigation for plant feedback at a particular level was significantly smaller than the irrigation for common practice at the corresponding irrigation level. For both crops in 2021, the seasonal irrigation for the plant feedback with over level was smaller than the common practice with full level. The rainfed crop in 2021 produced similar yield as irrigated crop. The crop yield in 2021 had a small range between different method-level plots due to the smaller irrigation applied in 2021 as compared with 2020.

Overall, the crop yield was similar among majority of the treatments implemented in the study for both years. The rainfed maize had a significantly lower yield than the irrigated treatments in 2020. The deficit irrigation applied at 50% produced largest IWP for both crops and no significant reduction in yield was observed for this level during the two growing seasons. However, the seasonal irrigation prescribed using the different methods was substantially different from each other. The ISSCADA plant feedback method prescribed the least irrigation depth among the methods in two crop-year cases. The ISSCADA hybrid and SETMI methods also prescribed the least irrigation in one of the four crop-year scenarios while maintaining optimal crop yield. This demonstrates that the two ISSCADA and SETMI methods performed well by reducing irrigation applications over the common practice method while producing adequate yield. Further studies are warranted to test these methods in arid and other climates. The iCWSI thresholds developed for this field should be further validated for irrigation management in the sub-humid climate of the Central Great Plains by continuing irrigation scheduling using these thresholds on two or more growing seasons for maize and soybean.

Comparative usability of SETMI and ISSCADA

Both decision support systems differ from each other in terms of ease of use, cost, labor requirements, transferability, and viability for adoption. These systems were used in the sub-humid climate of eastern Nebraska in this study. The SETMI model has been implemented for site-specific irrigation scheduling in Nebraska for about 8 years (Barker et al., 2018, 2019; Bhatti et al., 2020). The ISSCADA system was also tested in many different locations with different climates in the US (Evelt et al., 2020b; O’Shaughnessy et al., 2015, 2017; Stone et al., 2020; Vories et al., 2020). Significant reductions in prescribed irrigation depth were observed in the previous studies using these irrigation scheduling methods as compared with the conventional methods. The SETMI model can be implemented for irrigation scheduling using freely available satellite data as compared to the ISSCADA system which has a considerable initial investment (~US\$10,000–15,000). The ISSCADA system requires extensive instrumentation including network of IRTs, soil water sensors, local weather station, radio enabled communication devices, embedded computer, weatherproof enclosures, and data loggers.

In terms of usability and time requirements, the SETMI model requires an expert user and significant time to run the model. It is currently not designed to be used by producers directly, but the model can be used by irrigation consultants to provide recommendations to the producers. Additionally, SETMI can forecast irrigation recommendations for a certain number of days in the future which allows producers to be better prepared for satisfying crop water needs. On the other hand, the ISSCADA system is capable of automation and designed to be used directly by producers. ISSCADA require farmers to run a dry scan each time a new irrigation prescription needs to be generated. However, this system can be automated to collect data, control the irrigation system, analyze data to design irrigation

recommendations, and apply water with no or minimal user inputs. With a remote desktop connection, the user can monitor and control the status of the center pivot through the ISS-CADA system. The soil water and spatial crop water stress data can be viewed with ease using the ARS-Pivot software which provide insights about different parts of the field. The ability to detect energy-limiting water stress (and use it to manage irrigation) before the crop canopy transitions to carbon-dioxide-limiting water stress and subsequent yield loss (Bhatti et al., 2022a) supports the idea of using thermal stress detection for a broad array of situations, including full irrigation as well as deficit irrigation. In terms of transferability, the SETMI model can be implemented in different locations and climates with relative ease. This is due to the widespread coverage of land cover by satellites with high temporal and spatial resolution. However, the ISSCADA system requires development of iCWSI thresholds in the new location which requires implementation of the system for at least one season for data collection. Both decision support systems have immense potential for precision irrigation, and their pros and cons should be considered before adopting a particular system for irrigation scheduling.

Implications for sensors on the pivot vs. unmanned aircraft systems

Although this study did not include unmanned aircraft systems (UAS), there is a growing interest in UAS for irrigation (Chavez et al., 2020); therefore, it is helpful to put the findings of this research in the context of irrigation management techniques using UAS. This study demonstrated that IRTs mounted on a pivot were successful in determining the spatial canopy temperature and crop water stress accurately. The moving irrigation systems can be additionally used to mount different sensors including multispectral sensors, RGB cameras, and thermal cameras. These irrigation systems can be used to collect data in windy conditions and has low cost of operation. The cost of electrical energy consumed during a dry scan was about \$3.60 for the pivot used in this study (Bhatti et al., 2022b). The data collection using sensors on these irrigation systems has potential for automation and does not require any labor for their operation. Currently, there are center pivots that can complete a revolution of a quarter section field (~60 ha) in only 90 min. This is significant as the data across the field can be collected from the moving irrigation systems with consistent weather conditions and time of day. The sensor data does not need to be corrected for atmospheric interference. Relatively low-cost UAS are available for capturing qualitative spatial patterns in crop canopy. However, UAS with a thermal sensor for canopy temperature are both costly and labor intensive, especially if accurate canopy temperature is needed (i.e., to calculate iCWSI). Maguire et al. (2021) highlight some of the challenges of accurately measuring canopy temperature with UAS (RMSE of 2.24 °C when evaluating UAS canopy temperature against canopy temperature from proximal IRTs). The UAS are operated under strict federal regulations and requires expert training on their effective operation. Additionally, some UAS are not recommended to be flown in windy conditions and require calm, sunny days for flying. The data collected from the UAS may require corrections on the captured imagery to account for atmospheric interference (Maguire et al., 2022).

The sensors on a pivot determine crop and field characteristics with considerable spatial coverage across the field. While it is possible to mount ample number of sensors on an irrigation system, the associated cost increases considerably with the addition of instrumentation. It is crucial to determine the minimum number of sensors needed for monitoring crop water stress and manage a field. The ISSCADA system can be used with a minimum of two

IRTs to cancel for sun angles as the pivot moves around the field. This would be sufficient for managing the entire field uniformly if the sensors were mounted on the outer two spans. Mounting sensors on the outer spans will increase the area sensed and improve confidence in irrigation decision making. However, it will be beneficial to use two pairs of IRTs in the outer two spans of the center pivot for managing variable rate irrigation (either speed or zone control). Instead of mounting all four sensors on the two outer spans, one pair of IRTs can also be used in an area with low yielding crop. On the contrary, the UAS can be maneuvered to collect data from all parts of the field with only one sensor.

Conclusions

This experiment implemented two scientific decision support systems for irrigation management of maize and soybean during the growing seasons of 2020 and 2021. The rainfall received during 2021 (386 mm) was about two times the amount received in 2020 (178 mm). The differences in crop yield were mainly observed between rainfed and irrigated methods in 2020 for both crops since 2020 was a dry year. The deficit level performed adequately and had no yield reduction (not significantly different with a 5% significance level) as compared to the full irrigation level. The irrigation prescribed was minimum for the plant feedback method in majority of crop-year combinations. With the exception of soybean in 2020, the ISSCADA hybrid and SETMI methods significantly reduced irrigation applications for both crops as compared with the common practice method while maintaining optimal yield. In 2021, the common practice method (127 mm for maize and 102 mm for soybean) prescribed more than double the irrigation amount as was prescribed by the plant feedback method (59 mm for maize and 46 mm for soybean). The deficit level had the largest IWP for both crops in 2020 and 2021. The SETMI model and ISSCADA system performed adequately by producing optimal yield while reducing irrigation applications as compared with the common practice. The newly developed thresholds for ISSCADA performed well by reducing irrigation applications over the common practice method in 2021 and producing optimal yield. Future research could update these thresholds with additional iCWSI data and test these thresholds in additional growing seasons with more weather variability.

Acknowledgements The authors acknowledge the Irrigation Innovation Consortium, Valmont Industries, and the Robert B. Daugherty Water for Food Global Institute at the University of Nebraska for their financial support. Mr. Mark Schroeder and his team from the University of Nebraska's Eastern Nebraska Research and Extension Center were very cooperative and helpful with the field operations. We also acknowledge personnel from the Biological Systems Engineering Department at the University of Nebraska-Lincoln for their support and help throughout the experiment. The weather data was accessed from the Automated Weather Data Network of the High Plains Regional Climate Center. The authors also thank Dr. Kent Eskridge for his expertise and assistance in designing the experiment and conducting the statistical analyses. The authors are also grateful for Mr. Pradhyun Kashyap who reviewed an earlier version of this manuscript.

Funding Funding was received by the Irrigation Innovation Consortium under project title "Toward Pivot Automation with Proximal Sensing," including match funding from Valmont Industries, Inc. The ISSCADA system was patented by USDA-ARS (Evelt, O'Shaughnessy, and Peters), US 8,924,031 B1, Dec. 30, 2014, and licensed by Valmont Industries, Inc., in July 2018.

Declarations

Conflict of interest The authors declare that they have no other known competing financial interests that could have appeared to influence the work reported in this paper.

Open Access This article is licensed under a Creative Commons Attribution 4.0 International License, which permits use, sharing, adaptation, distribution and reproduction in any medium or format, as long as you give appropriate credit to the original author(s) and the source, provide a link to the Creative Commons licence, and indicate if changes were made. The images or other third party material in this article are included in the article's Creative Commons licence, unless indicated otherwise in a credit line to the material. If material is not included in the article's Creative Commons licence and your intended use is not permitted by statutory regulation or exceeds the permitted use, you will need to obtain permission directly from the copyright holder. To view a copy of this licence, visit <http://creativecommons.org/licenses/by/4.0/>.

References


- Allen, R. G., Pereira, L. S., Raes, D., Smith, M., (1998). Crop evapotranspiration: Guidelines for computing crop water requirements, Irrigation and drainage paper 56, *Food and Agriculture Organization of the United Nations*.
- Andrade, M. A., Shaughnessy, S. A. O., & Evett, S. R. (2020). ARSPIVOT, a sensor-based decision support software for variable-rate irrigation center pivot systems: Part A. Development. *Transactions of the ASABE*, 63, 1521–1533. <https://doi.org/10.13031/trans.13907>
- Barker, J. B., Bhatti, S., Heeren, D. M., Neale, C. M. U., & Rudnick, D. R. (2019). Variable rate irrigation of maize and soybean in west-central nebraska under full and deficit irrigation. *Frontiers in Big Data*, 2, 1–15. <https://doi.org/10.3389/fdata.2019.00034>
- Barker, J. B., Heeren, D. M., Neale, C. M. U., & Rudnick, D. R. (2018). Evaluation of variable rate irrigation using a remote-sensing-based model. *Agricultural Water Management*, 203, 63–74. <https://doi.org/10.1016/j.agwat.2018.02.022>
- Bhatti, S., Heeren, D. M., Barker, J. B., Neale, C. M. U., Woldt, W. E., Maguire, M. S., & Rudnick, D. R. (2020). Site-specific irrigation management in a sub-humid climate using a spatial evapotranspiration model with satellite and airborne imagery. *Agricultural Water Management*, 230, 105950. <https://doi.org/10.1016/j.agwat.2019.105950>
- Bhatti, S., Heeren, D. M., Evett, S. R., O'Shaughnessy, S. A., Rudnick, D. R., Franz, T. E., Ge, Y., & Neale, C. M. U. (2022a). Crop response to thermal stress without yield loss in irrigated maize and soybean in Nebraska. *Agricultural Water Management*, 274, 107946. <https://doi.org/10.1016/j.agwat.2022.107946>
- Bhatti, S., Heeren, D. M., Shaughnessy, S. A. O., Evett, S. R., Maguire, M. S., Kashyap, S. P., & Neale, C. M. U. (2022b). Comparison of stationary and mobile canopy sensing systems for maize and soybean in Nebraska, USA. *Applied Engineering in Agriculture*, 38, 331–342. <https://doi.org/10.13031/aea.14945>
- Campos, I., Neale, C. M. U., Suyker, A. E., Arkebauer, T. J., & Gonçalves, I. Z. (2017). Reflectance-based crop coefficients REDUX: For operational evapotranspiration estimates in the age of high producing hybrid varieties. *Agricultural Water Management*, 187, 140–153. <https://doi.org/10.1016/j.agwat.2017.03.022>
- Chavez, J. L., Torres-Rua, A. F., Woldt, W. E., Zhang, H., Robertson, C., Marek, G. W., Wang, D., Heeren, D. M., Taghvaeian, S., & Neale, C. M. U. (2020). A decade of unmanned aerial systems in irrigated agriculture in the Western US. *Applied Engineering in Agriculture*, 36(4), 423–436. <https://doi.org/10.13031/aea.13941>
- Eisenhauer, D. E., Martin, D. L., Heeren, D. M., Hoffman, G. J., 2021. Irrigation system management, *ASABE*. ASABE, St. Joseph, Michigan. <https://doi.org/10.13031/ISM.2021>
- Evans, R. G., LaRue, J., Stone, K. C., & King, B. A. (2013). Adoption of site-specific variable rate sprinkler irrigation systems. *Irrigation Science*, 31, 871–887. <https://doi.org/10.1007/s00271-012-0365-x>
- Evett, S. R., O'Shaughnessy, S. A., Peters, R. T., 2014. Irrigation scheduling and supervisory control and data acquisition system for moving and static irrigation systems. *US Patent* 8,924,031.
- Evett, S. R., Andrade, M. A., Anderson, M. C., & Thompson, A. (2020a). Precision agriculture and irrigation: Current US. *Perspectives. Transactions of the ASABE*, 63, 57–67.
- Evett, S. R., Colaizzi, P. D., Lamm, F. R., O'Shaughnessy, S. A., Heeren, D. M., Trout, T. J., Kranz, W. L., & Lin, X. (2020b). Past, present, and future of irrigation on the US great plains. *Transactions of the ASABE*. <https://doi.org/10.13031/TRANS.13620>
- Evett, S. R., Shaughnessy, S. A. O., Andrade, M. A., & Colaizzi, P. D. (2020c). Theory and development of a vri decision support system: The usda-ars isscada approach. *Transactions of the ASABE*, 63, 1507–1519.
- Geli, H. M. E., Neale, C. M. U., (2012) Spatial evapotranspiration modelling interface (SETMI), in: *Remote Sensing and Hydrology*. pp. 171–174.

- Haghverdi, A., Leib, B. G., Washington-Allen, R. A., Buschermohle, M. J., & Ayers, P. D. (2016). Studying uniform and variable rate center pivot irrigation strategies with the aid of site-specific water production functions. *Computer and Electronics in Agriculture*, *123*, 327–340. <https://doi.org/10.1016/j.compag.2016.03.010>
- Huete, A. R. (1988). A soil-adjusted vegetation index (SAVI). *Remote Sensing of Environment*, *25*, 295–309. [https://doi.org/10.1016/0034-4257\(88\)90106-X](https://doi.org/10.1016/0034-4257(88)90106-X)
- Jackson, R. D., Idso, S. B., Reginato, R. J., & Pinter, P. J., Jr. (1981). Canopy temperature as a crop water stress indicator. *Water Resources Research*, *17*, 1133–1138. <https://doi.org/10.1029/WR017i004p01133>
- Koester, R. P., Nohl, B. M., Diers, B. W., & Ainsworth, E. A. (2016). Has photosynthetic capacity increased with 80 years of soybean breeding? An examination of historical soybean cultivars. *Plant, Cell and Environment*, *39*, 1058–1067. <https://doi.org/10.1111/pce.12675>
- Lena, B. P., Ortiz, B. V., Jiménez-López, A. F., Sanz-Sáez, Á., O’Shaughnessy, S. A., Durstock, M. K., & Pate, G. (2020). Evaluation of infrared canopy temperature data in relation to soil water-based irrigation scheduling in a humid subtropical climate. *Transactions of the ASABE*, *65*, 1217–1231. <https://doi.org/10.13031/TRANS.13912>
- Lo, T., Heeren, D. M., Martin, D. L., Mateos, L., Luck, J. D., & Eisenhauer, D. E. (2016). Pumpage reduction by using variable-rate irrigation to mine undepleted soil water. *Transactions of the ASABE*, *59*, 1285–1298. <https://doi.org/10.13031/trans.59.11773>
- Maguire, M. S., Neale, C. M. U., & Woldt, W. E. (2021). Improving accuracy of unmanned aerial system thermal infrared remote sensing for use in energy balance models in agriculture applications. *Remote Sensing*, *13*(9), 1635. <https://doi.org/10.3390/rs13091635>
- Maguire, M. S., Neale, C. M. U., Woldt, W. E., & Heeren, D. M. (2022). Managing spatial irrigation using remote-sensing-based evapotranspiration and soil water adaptive control model. *Agricultural Water Management*. <https://doi.org/10.1016/j.agwat.2022.107838>
- Mendes, W. R., Araújo, F. M. U., Dutta, R., & Heeren, D. M. (2019). Fuzzy control system for variable rate irrigation using remote sensing. *Expert Systems with Applications*, *124*, 13–24. <https://doi.org/10.1016/j.eswa.2019.01.043>
- Neale, C. M. U., Geli, H. M. E., Kustas, W. P., Alfieri, J. G., Gowda, P. H., Evett, S. R., Prueger, J. H., Hipps, L. E., Dulaney, W. P., Chávez, J. L., French, A. N., & Howell, T. A. (2012). Soil water content estimation using a remote sensing based hybrid evapotranspiration modeling approach. *Advances in Water Resources*, *50*, 152–161. <https://doi.org/10.1016/j.advwatres.2012.10.008>
- Norman, J. M., Kustas, W. P., & Humes, K. S. (1995). Source approach for estimating soil and vegetation energy fluxes in observations of directional radiometric surface temperature. *Agricultural and Forest Meteorology*, *77*, 263–293. [https://doi.org/10.1016/0168-1923\(95\)02265-Y](https://doi.org/10.1016/0168-1923(95)02265-Y)
- O’Shaughnessy, S. A., Andrade, M. A., & Evett, S. R. (2017). Using an integrated crop water stress index for irrigation scheduling of two corn hybrids in a semi-arid region. *Irrigation Science*, *35*, 451–467. <https://doi.org/10.1007/s00271-017-0552-x>
- O’Shaughnessy, S. A., Evett, S. R., & Colaizzi, P. D. (2015). Dynamic prescription maps for site-specific variable rate irrigation of cotton. *Agricultural Water Management*, *159*, 123–138. <https://doi.org/10.1016/j.agwat.2015.06.001>
- O’Shaughnessy, S. A., Evett, S. R., Colaizzi, P. D., Andrade, M. A., Marek, T. H., Heeren, D. M., Lamm, F. R., & LaRue, J. L. (2019). Identifying advantages and disadvantages of variable rate irrigation: An updated review. *Applied Engineering in Agriculture*, *35*, 837–852. <https://doi.org/10.13031/aea.13128837>
- O’Shaughnessy, S. A., Evett, S. R., Colaizzi, P. D., & Howell, T. A. (2012). A crop water stress index and time threshold for automatic irrigation scheduling of grain sorghum. *Agricultural Water Management*, *107*, 122–132. <https://doi.org/10.1016/j.agwat.2012.01.018>
- O’Shaughnessy, S. A., Kim, M., Andrade, M. A., Colaizzi, P. D., & Evett, S. R. (2020). Site-specific irrigation of grain sorghum using plant and soil water sensing feedback—Texas High Plains. *Agricultural Water Management*, *240*, 106273. <https://doi.org/10.1016/j.agwat.2020.106273>
- Osroosh, Y., Peters, R. T., Campbell, C. S., & Zhang, Q. (2016). Comparison of irrigation automation algorithms for drip-irrigated apple trees. *Computer and Electronics in Agriculture*, *128*, 87–99. <https://doi.org/10.1016/j.compag.2016.08.013>
- Peters, R. T., & Evett, S. R. (2004). Modeling diurnal canopy temperature dynamics using one-time-of-day measurements and a reference temperature curve. *Agronomy Journal*, *96*, 1553–1561. <https://doi.org/10.2134/agronj2004.1553>
- Stone, K. C., Bauer, P. J., O’Shaughnessy, S., Andrade-Rodriguez, A., & Evett, S. (2020). A variable-rate irrigation decision support system for corn in the US Eastern Coastal plain. *Transactions of the ASABE*, *65*, 1295–1303. <https://doi.org/10.13031/TRANS.13965>

- Sui, R., O’Shaughnessy, S., Evett, S. R., Andrade-Rodriguez, A., & Baggard, J. (2020). Evaluation of a decision support systems for variable-rate irrigation in a humid region. *Transactions of the ASABE*, *125*, 17–35.
- Sui, R., & Yan, H. (2017). Field study of variable rate irrigation management in humid climates. *Irrigation and Drainage*, *66*, 327–339. <https://doi.org/10.1002/ird.2111>
- Taghvaeian, S., Comas, L., DeJonge, K. C., & Trout, T. J. (2014). Conventional and simplified canopy temperature indices predict water stress in sunflower. *Agricultural Water Management*, *144*, 69–80. <https://doi.org/10.1016/j.agwat.2014.06.003>
- Thorp, K. R. (2020). Long-term simulations of site-specific irrigation management for Arizona cotton production. *Irrigation Science*, *38*, 49–64. <https://doi.org/10.1007/s00271-019-00650-6>
- Thorp, K. R., Calleja, S., Pauli, D., Thompson, A. L., & Elshikha, D. E. (2022). Agronomic outcomes of precision irrigation management technologies with varying complexity. *Journal of the ASABE*, *65*, 135–150. <https://doi.org/10.13031/ja.14950>
- Vories, E., O’Shaughnessy, S., Sudduth, K., Evett, S., Andrade, M., & Drummond, S. (2020). Comparison of precision and conventional irrigation management of cotton and impact of soil texture. *Precision Agriculture*. <https://doi.org/10.1007/s11119-020-09741-3>
- Zhang, J., Guan, K., Peng, B., Pan, M., Zhou, W., Jiang, C., Kimm, H., Franz, T. E., Grant, R. F., Yang, Y., Rudnick, D. R., Heeren, D. M., Suyker, A. E., Bauerle, W. L., & Miner, G. L. (2021). Sustainable irrigation based on co-regulation of soil water supply and atmospheric evaporative demand. *Nature Communications*, *12*, 1–10. <https://doi.org/10.1038/s41467-021-25254-7>

Publisher’s Note Springer Nature remains neutral with regard to jurisdictional claims in published maps and institutional affiliations.

Authors and Affiliations

Sandeep Bhatti¹ · Derek M. Heeren²  · Susan A. O’Shaughnessy³ · Christopher M. U. Neale⁴ · Jacob LaRue^{5,6} · Steve Melvin⁷ · Eric Wilkening² · Geng Bai²

✉ Derek M. Heeren
derek.heeren@unl.edu

¹ University of Massachusetts Cranberry Station, 1 State Bog Road, East Wareham, MA 02538, USA

² Department of Biological Systems Engineering, University of Nebraska-Lincoln, 3605 Fair St., Lincoln, NE 68583, USA

³ USDA-ARS Conservation and Production Research Laboratory, 2300 Experiment Station Rd, Bushland, TX 79012, USA

⁴ Daugherty Water for Food Global Institute at the University of Nebraska, 2021 Transformation Drive, Suite 3220, Lincoln, NE 68508, USA

⁵ Owasso, OK, USA

⁶ Formerly Valmont Industries, Inc., Omaha, NE 68154, USA

⁷ Nebraska Extension, 1784 Fairgrounds Rd., Central City, NE 68826, USA